# Treatment of high strength industrial wastewater with membrane bioreactors for water reuse: effect of pre-treatment with aerobic granular sludge on system performance and fouling tendency

**Daniele Di Trapani[a], Santo Fabio Corsino[a,*], Michele Torregrossa[a], Gaspare Viviani[a]**

[a] Dipartimento di Ingegneria, Università di Palermo, Viale delle Scienze, 90128 Palermo, Italy

*Corresponding author: tel: +39 09123896555; fax: +39 09123860810

E-mail address: santofabio.corsino@unipa.it (Santo Fabio Corsino)

## Abstract

In this study, the treatment of citrus wastewater with membrane bioreactors (MBRs) under different configurations was investigated for water reuse. In particular, one MBR and one aerobic granular sludge MBR (AGS+MBR) bench scale plants were operated for 60 days. The experimental campaign was divided into two periods. In Phase I, a conventional hollow fiber MBR was employed for the treatment of the raw high strength wastewater, whereas in Phase II a combination of in-series reactors (AGS plus MBR) was adopted for the treatment of the high strength citrus wastewater

The results demonstrated that both plant configurations enabled very high COD removal, with average values close to 99%. Respirometric batch tests revealed a considerable high metabolic activity of the biomass in both plant configurations, with higher values in the AGS+MBR. It was speculated that the MBR reactor enriched in active biomass deriving from the erosion of the external granule layers in the upstream reactor. In terms of fouling tendency, higher resistance to filtration was observed in the AGS+MBR plant, also characterized by higher irremovable resistance increase compared to the MBR plant that might severely affect the membrane service life.



**Keywords:** Resistance-In-Series model; fouling tendency; aerobic granular sludge; biokinetics; citrus wastewater; Membrane Bioreactor

## 1. Introduction

The citrus processing industry requires high water amounts for washing the fruits and the machinery, for the extraction of juice and essential oils (EO) from the fruits, as well as for floor washing, peel drying and cooling [1,2]. These operations produce as a consequence high amount of wastewater (characterized by high organic content) that represents a great concern nowadays [3,4]. Studies revealed that a citrus factory processing 25 t $h^{-1}$ of lemons might produce more than 10 million litres of wastewater per day [5]. Citrus wastewater is usually characterized by high content of organic matter, suspended solids and EO. Wastewater from citrus processing is characterized by seasonal variability in quality and quantities, high acidity and unbalanced nutrients content due to the limiting concentrations of nitrogen and phosphorous [6]. Indeed, chemical oxygen demand (COD) concentration is characterized by huge variations according to the different stages of the production process that reach its highest peak at March beginning [1]. Moreover, the quality characteristics of citrus wastewater might show significant fluctuations even in the workday, depending on the production step. EOs are known to be antimicrobial, thus their presence should limit the biological processes, even at low concentrations [1]. As general comment, the composition and the huge quality variations pose a serious challenge for biological systems, referring in particular to conventional activated sludge (CAS) systems. Therefore, the compliance with more severe restrictions for discharging in the sewer facility or into receiving water bodies requires advanced technologies enabling efficient treatment of citrus wastewater. Moreover, it is encouraged to propose a low-footprint technology that is suitable for the on-site treatment of wastewaters produced by the same industry. In this context, it is also desirable to implement an advanced and highly performing system with the aim to obtain water with quality that complies with the requirements of the European Directive 98/83/EC [7], for the reuse of the treated wastewater inside the production process. This solution is indeed needed from both the environmental and economical sustainability [3].

Several technologies have been proposed in the literature for the treatment of citrus wastewater [8]. Among these, conventional activated sludge (CAS) system, although its reliability, is related to a highly energy-consuming process [5]. Moreover, because of the high amount of readily biodegradable organic matter contained in citrus wastewaters, the overgrowth of several filamentous bacteria species is favored, thereby causing the occurrence of bulking or foaming phenomena. To overcome these drawbacks, some authors proposed aerated lagooning systems [1]. The aerated ponds offer the advantage to require low-intensity aeration and do not require the settling phase. However, very large areas are required to treat high-strength wastewater with such system.

In recent years, membrane bioreactors (MBRs) have attracted growing interest and they have been widely applied for the treatment of municipal as well as industrial wastewater [9,10]. Basically, MBR applies to wastewater treatment processes that integrate a perm-selective membrane with a biological process for the final solid-liquid separation [11]. In particular, MBR have demonstrated to be excellent in solid-liquid separation, also providing very good effluent quality coupled with high sludge retention time (SRT) values, volumetric loading rates and low footprint requirements [11,12]. MBRs, because of the higher capacity of solid retention compared with CAS system, allow operating with higher biomass concentration, thus giving the possibility to operate with smaller volume reactors and providing low footprint requirement. Moreover, MBRs enable the achievement of very high permeate quality that is suitable for on-site reutilization. This could promote cleaner and more sustainable management operations of the citrus processing industries.

Nevertheless, the main drawback associated with MBR operations is represented by membrane fouling [13,14], still hampering the world-wide application of MBRs. Basically, the membrane permeability is strongly influenced by external deposition, referred to as cake layer, as well as internal fouling, usually referred to as pore blocking [9]. The high energy consumption due to membrane aeration (needed to mitigate the extent of membrane fouling), represents another significant drawback of MBRs [15].

The high strength characterizing citrus wastewater coupled to its significant quality fluctuations can determine a worsening of sludge features thus promoting severe membrane fouling [16]. Therefore, a pre-treatment of citrus wastewater might be proposed prior to MBR operation. In this light, the joint application of aerobic granular sludge (AGS) technology and MBRs could represent one of the most attractive solution for a proper management of this kind of wastewater. AGS have been successfully implemented for the treatment of both municipal and industrial wastewater. The literature studies demonstrated that aerobic granules feature a compact and thick structure, thus ensuring a great ability to withstand adverse environmental conditions, such as loading variation, obtaining very high effluent quality at the same time [17–20]. Indeed, the granular sludge features very high settling ability and allows to maintain higher biomass concentrations, thus reducing the plant footprint [21]. However, when treating high strength industrial wastewaters rich in particulate organic matter, the granules might turn into filamentous structure, due to the proliferation of fast-growing bacteria [20]. In this situation, granules may result prone to breakage and degranulation might occur thus leading to a release of extracellular polymeric substances (EPS) that have been recognized to be one of the most important foulant agents for MBR [22]. Seeding the AGS within a MBR in a combined AGS+MBR system was already studied in the literature [23,24]. The results demonstrated that structural instability of AGS promoted a severe membrane fouling. In this light, due to the AGS intrinsic instability when treating high strength wastewater, operating a system that integrates AGS+MBR within a single reactor is not advisable for treating industrial wastewater.

Nevertheless, the in-series combination between AGS and MBR appears undoubtedly a very promising solution for the treatment of high strength industrial wastewater, in order to enhance system compactness as well as energy saving for the operation of the membrane compartment. Indeed, the ability of AGS to withstand high organic loading rates coupled to the high-quality effluent (free of particulate matter) of MBRs makes this combination attractive [25]. Therefore, system configurations involving the coupling of AGS and MBR in separate compartments should be examined, also due to the lack of knowledge on this topic. Indeed, to authors' knowledge, in the technical literature no studies were reported on the coupling of AGS and MBR technology in separated reactors placed in-series for the treatment of high strength citrus wastewater.

Bearing in mind the above considerations, the aim of the present work is to get insights about the treatment of high strength citrus wastewater with two MBR configurations, involving one conventional MBR and one in-series AGS+MBR bench scale plants. In particular, the main targets of the present study were: (i) analyse the main features of membrane fouling for the investigated configurations; (ii) assess the biological removal performance at different organic loading rates. It is worth noting that this study represents a preliminary investigation aimed at exploring the potential application of these configurations in a real citrus processing industry.

## 2. Materials and methods

### *2.1 MBR and AGS+MBR plant configuration*

As aforementioned, in the present study two different MBR configurations were investigated for the treatment of high strength citrus wastewater, the first one being a conventional MBR, while the second one was an AGS+MBR configuration. The MBR bench scale plant consisted of one aerobic reactor (20 L of volume) equipped with fine bubble air diffusers. An ultrafiltration (UF) hollow fiber (HF) membrane module (Zee-Weed®01, courtesy of GE), with specific area equal to 0.1 $m^2$ and nominal porosity of 0.04 μm (height: 20 cm, external diameter: 6 cm) was placed within the reactor in submerged configuration for permeate extraction. The permeate flux was kept to approximately 12.5 L $m^{-2}h^{-1}$, thereby corresponding to a net permeate flow rate of 0.63 L $h^{-1}$. Therefore, the average hydraulic retention time (HRT) of the system was of approximately 31 h, in line with previous studies [26]. The AGS+MBR bench scale plant was composed by two identical aerobic granular sludge sequencing batch reactors (AGSBRs) (namely, R1 and R2) in-series with the MBR compartment. In particular, each AGSBR was characterized by an overall 5 L volume with a of 4 L working volume. They were column shaped reactors (height: 100 cm) characterized by inner diameter of 8.6 cm equipped with a riser (height: 50 cm; internal diameter: 5.4 cm). Oxygen was provided to the reactors through a fine bubble diffuser placed at the bottom of each reactor with an air flow rate of 3 L $min^{-1}$, corresponding to up-flow air velocity of 2.4 cm $s^{-1}$. The latter values were in good agreement with previous experiments on AGS [27,28]. The AGSBRs effluent was stored in a tank that served as balancing volume between the discontinuous flow regime of the AGSBRs and the continuous flow of the MBR. Subsequently, the effluent of both the AGSBRs was fed to the MBR compartment. Nevertheless, in this case, permeate flux was kept to approximately 10 L $m^{-2}$ $h^{-1}$ with the aim to lowering the membrane fouling development, while the net effluent flow rate was equal to 0.4 L $h^{-1}$. It is worth noting that the granules were retained inside the column-shaped reactors, while the sloughed-biomass contained in the effluent supernatant arrived to the MBR compartment.

In both MBR configurations, the membrane filtration cycle was divided into 5 min of filtration and 1 min of backwashing. When the transmembrane pressure (TMP) reached 0.6-0.7 bar (basing on the Manufacturer advice), the filtration cycle was interrupted and subsequently the membrane module was subjected to either physical or chemical cleanings. Figure 1 reports a schematic layout of the investigated MBR configurations.

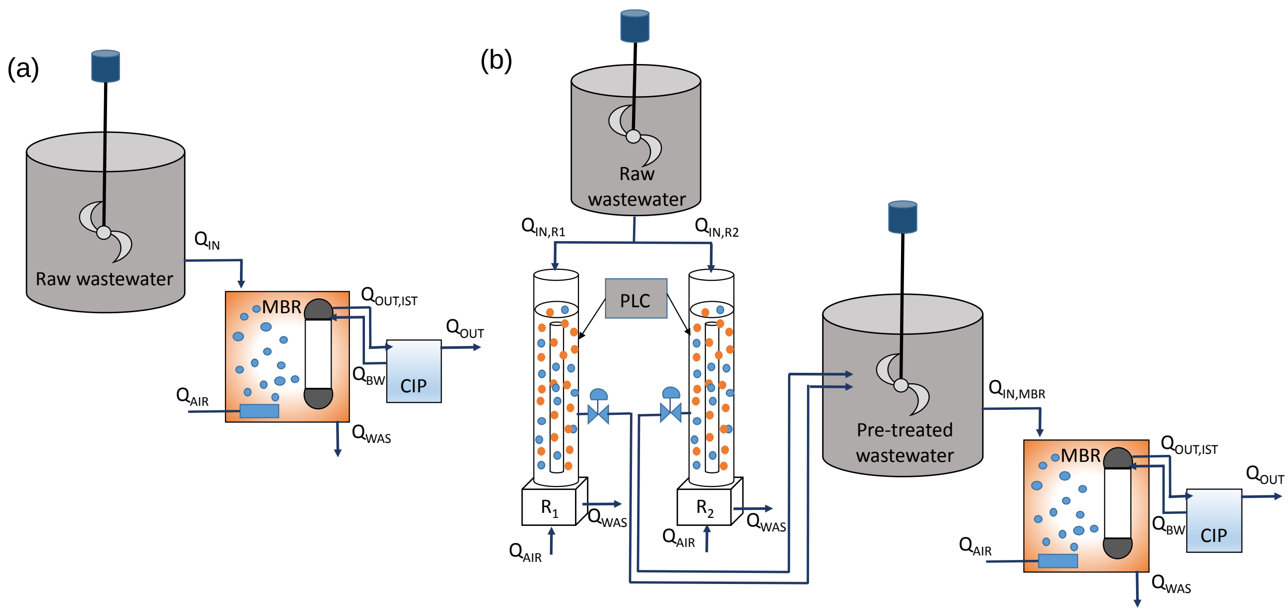


**Figure 1.** Schematic lay-out of (a) MBR and (b) in-series AGS+MBR configurations.

*2.2 Experimental campaign*

The experimental campaign was divided into two phases (namely, Phase I and Phase II) and it was characterized by an overall duration of about 60 days. During Phase I, a conventional MBR bench scale plant was operated for 35 days, with an average flow rate of approximately 15.1 L $d^{-1}$. During Phase II, the reactor configuration was changed to an in-series AGS+MBR treatment line. The bench scale plant was operated with this configuration for 25 days with an average flow rate of approximately 10 L $d^{-1}$. The AGSBRs operated with a cycle duration of 6 hours. In detail, the SBR cycle of the AGS reactors was distributed as follows: 10 minutes of feeding, 340 minutes of aeration 5 minutes of settling and 5 minutes of effluent withdrawal. The volume of the raw wastewater treated per day by the AGSBRs was equal to 16 L.

Throughout experiments both plants were fed with real citrus wastewater (pH=5.2±0.2). Because the raw citrus wastewater lacked nutrients, nitrogen ($NH_4Cl$) and phosphorous ($KH_2PO_4$) were added according to the COD of the wastewater to maintain a nutrient ratio of 200 COD: 5 N: 1 P by weight, in order to avoid heterotrophic growth limitation. The main features of the influent wastewater as well as the main operational conditions during experiments are summarized in Table 1. Referring to the C/N ratio of the feeding wastewater, it is expressed in terms of soluble COD (SCOD), i.e. after wastewater filtration at 0.45 μm. It is worth mentioning that the present work is specifically focused on the performance of the MBR compartment; therefore, further details about the AGSBR reactors description as well as the granular sludge performance results can be found elsewhere [2].

**Table1.** Main characteristics of the raw wastewater as well as operational conditions (in brackets the standard deviation values)

| Parameter | Units | Phase I | Phase II | |
|---|---|---|---|---|
| | | MBR | AGS (R1-R2) | MBR |
| Total COD (TCOD) | mg $L^{-1}$ | 5150 (±1130.7) | 5815.30 (±1939) | 1148.9 (±493.35) |
| Soluble COD (SCOD) | mg $L^{-1}$ | 3283 (±1398) | 3552.3 (±1609.5) | 614.6 (±333.4) |
| Total Nitrogen | mg $L^{-1}$ | 110 (±44) | 88 (±39) | 30.77 (±7.56) |
| Total Phosphorous | mg $L^{-1}$ | 20 (±5.7) | 17.6 (±4.31) | 6.25 (±3.92) |
| TSS | mg $L^{-1}$ | 885.71 (±321) | 1208.9 (±159.4) | 1613 (±272.06) |
| C/N ratio | mgSCOD $mg^{-1}$N | 29.85 | 40.36 | 19.97 |
| pH | - | 7.2±0.3 | 7.4±0.4<br>5.1±0.2 | 8.17 (±0.42) |
| Permeate Flux | L $m^{-2}$ $h^{-1}$ | 12.5 (±2.40) | - | 10 (±1.45) |
| Organic loading rate [OLR] | kgCOD $m^{-3}d^{-1}$ | 3.8 (±1.32) | 2.8 (±1.32) | 0.61 (±0.4) |
| Hydraulic Retention time [HRT] | [h] | 31.61 (±12.76) | 12 | 52.84 (±10.23) |

| | | | | |
|---|---|---|---|---|
| Sludge Retention Time [SRT] | [d] | 9.25 (±3.21) | 1.8 | 38.02 (±7.18) |

The MBR compartment was inoculated with activated sludge collected from the wastewater treatment plant (WWTP) of "Agrumaria Corleone S.p.A." with an initial total suspended solid (TSS) concentration of 6 g TSS $L^{-1}$. R1 was inoculated with mature aerobic granular sludge collected from a parent system, while R2 was inoculated with the waste sludge collected from reactor R1.

*2.3 Analytical methods*

All of the key compounds required to characterize the collected samples were analysed according to the Standard Methods [29]: COD, $BOD_5$, total phosphorus, TSS and volatile suspended solid (VSS) in the influent, effluent as well as in the mixed liquor (MLSS). Total COD (TCOD) was measured directly in the sample (supernatant), while the soluble COD (SCOD) was determined after filtration through a 0.45 µm membrane. Total nitrogen was measured by a TN analyzer (Shimadzu). Concerning the organic matter removal, with the aim to discriminate between the removal due to the bacterial consortium from the physical effect due to membrane filtration, the biological ($\eta_{BIO}$) and total ($\eta_{TOT}$) removal efficiency were assessed in agreement with Mannina et al. (2016).

The loosely bound EPS (LB-EPS), also including the soluble microbial products (SMPs), were obtained by centrifugation at 5000 rpm for 5 min, while the tightly bound EPS (TB-EPS) were extracted by means of the thermal extraction method (among others [13]). The extracted TB-EPS and the LB-EPS were then analysed for proteins by using the Folin method with bovine serum albumin as the standard [31], whilst the carbohydrates were measured according to [32], which yields results as glucose equivalent. Moreover, the sum of proteins and carbohydrates was considered as the total EPS content ($EPS_T$).

Both activated sludge and granules size distributions were measured by means of a high-speed image analyses sensor (Sympatec Qicpic) providing the particle size distribution as well as the granulometric curve. Basing on the granulometric curve, the uniformity coefficient (UC) was calculated as the $D_{60}$

to $D_{10}$ ratio, where $D_{60}$ and $D_{10}$ mean the diameter of the particles for which 60 percent and 10 percent respectively of the particles are smaller. The microscopic image observations were performed by a phase contrast microscope (BX-53-Olympus).

The specific observed heterotrophic yield coefficient ($Y_{obs}$) of the MBR compartment was evaluated through mass balances between sludge withdrawn, sludge production dividing by the COD removed, according to [33] (Eq. 1):

$$Y_{obs} = \frac{\Delta M_{VSS}}{\Delta COD_{rem}} \qquad [1]$$

where $\Delta COD_{rem}$ represents the cumulated COD removed, while $\Delta M_{VSS}$ represents the overall sludge production, given by:

$$\Delta M_{VSS} = x * Q_{WAS} + \Delta X * V_{MBR}\ [kgVSS\ d^{-1}] \qquad [2]$$

where $x$ represents the biomass concentration in the waste sludge stream, $Q_{WAS}$ is the waste sludge flow rate, $\Delta X$ the variation of the activated sludge concentration, $V_{MBR}$ is the volume of the MBR compartment.

Respirometric batch tests were carried out on wastewater and MBR biomass samples for the evaluation of the kinetic/stoichiometric parameters according to [34], as well as to assess the composition of the COD fractions, in agreement with previous experiences [2]. In the batch tests aimed at evaluating the heterotrophic biokinetic/stoichiometric parameters, the nitrifying biomass was inhibited by adding 10 mg $L^{-1}$ of Allylthiourea (ATU), while the exogenous oxygen uptake rate (OUR) was enhanced by the addition of a readily biodegradable organic substrate (sodium acetate in this case). Before starting each batch test, the biomass samples were aerated until endogenous conditions were reached, by monitoring the OUR values. The COD fractions, were classified as soluble readily biodegradable (Ss), soluble inert ($S_I$), biodegradable and rapidly hydrolysable (Xs), particulate inert ($X_I$) and active biomass (Xa), and were evaluated according to [2].

The membrane fouling was analysed by measuring the total resistance to filtration ($R_T$) according to the following equation:

$$R_T = \frac{TMP}{\mu \cdot J} \quad [3]$$

where, $R_T$ is the total resistance to filtration ($10^{12}$ $m^{-1}$), TMP is the transmembrane pressure (Pa), μ the permeate viscosity (Pa·s), and J the permeation flux (m $s^{-1}$).

The resistance-in-series (RIS) model was applied according to Di Bella et al. (2018), for the assessment of the specific mechanisms of deposition. Specifically, the RIS model allowed to evaluate the $R_T$ decomposition according to the following equation:

$$R_T = R_m + R_{PB} + R_{C,irr} + R_{C,rev} \quad [4]$$

where $R_m$ represents the intrinsic resistance of the new membrane, $R_{PB}$ the irreversible resistance due to particles deposition into the membrane pore (pore blocking), $R_{C,irr}$ the fouling resistance related to irreversible superficial cake deposition (removable with extraordinary physical cleaning), $R_{C,rev}$ the fouling resistance related to superficial cake deposition which is removed by ordinary backwashing.

Furthermore, membrane permeability ($K_{20}$) was calculated using a simple filtration model according to the following equation [35]:

$$K_{20} = \frac{J \cdot f_t}{TMP} \quad [5]$$

## 3. Results and discussions

As above mentioned, the thorough discussion of the AGS behaviour (including granules features and system performance) is reported elsewhere [2]. Briefly, the R1 and R2 reactors were operated under different OLR (from 3.0 kg TCOD $m^{-3}d^{-1}$ to 15 kg TCOD $m^{-3}d^{-1}$) and pH values (7.0 for R1 and 5.5 for R2). The achieved results highlighted COD removal almost of 90% in both reactors for OLR below 7 kg TCOD $m^{-3}d^{-1}$. For higher OLR values, it was observed a significant decrease of COD removal from 90% to less than 75% in R2, suggesting that the reactor operated with a pH of 5.5 was not able to withstand the COD removal with increasing OLR. Moreover, it was noticed a huge worsening of the granules physical properties with the increasing OLR, mainly due to unbalanced feast and famine phases, that favoured the proliferation of filamentous microorganisms.

*3.1 Organic carbon removal and COD fractionation results*

Figure 2 shows the influent and effluent COD concentrations, the COD removal efficiencies as well as the organic loading rates for the MBR (Figure 2a-b) and the AGS+MBR (Figure 2c-d) systems, respectively.

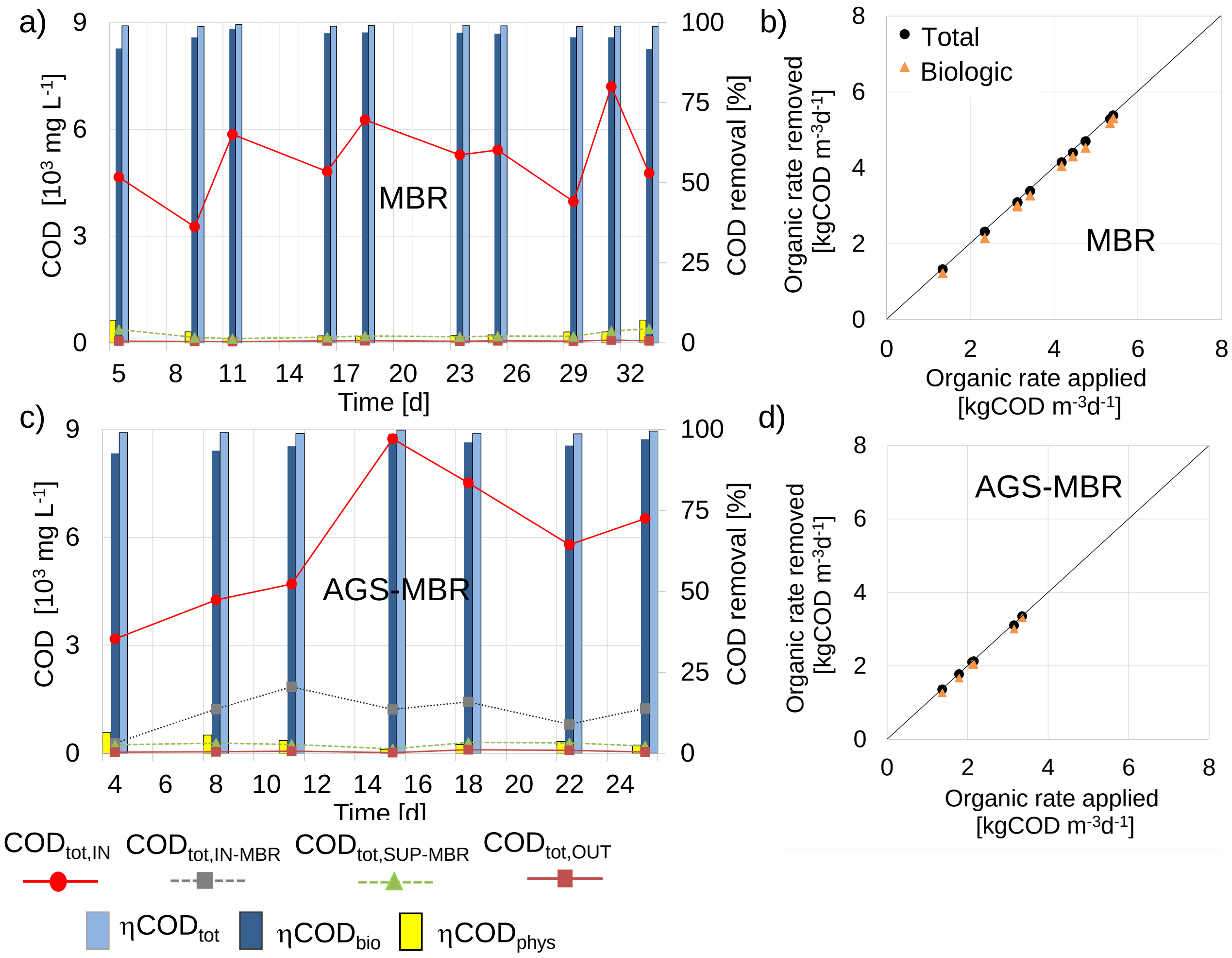


**Figure 2.** Influent, supernatant MLSS and permeate COD concentrations and removal efficiencies in Phase I (a); organic loading rate applied and removed in Phase I (b); influent, supernatant MLSS and permeate COD concentrations and removal efficiencies in Phase II (c) organic loading rate applied and removed in Phase II (d), respectively.

From the observation of data reported in Figure 2, it is worth noting that both configurations were able to provide an excellent COD removal, with total COD removal efficiency (as average) of 98.97 and 99.06% for MBR (Phase I) and AGS+MBR (Phase II), respectively. In particular, the COD concentrations in the permeate were 52.3 and 51.2 mg $L^{-1}$ in Phase I and II, respectively, thus highlighting the excellent quality of the treated water in terms of organic carbon content, potentially exploitable for water reuse. In terms of biological COD removal (i.e. before membrane filtration), the performance of both configurations was also very high, with average removal efficiency of 95.47 and 95.34% for MBR and AGS+MBR, respectively. Both configurations were able to remove almost completely the organic loading rates (OLRs) applied. Indeed, in the whole experiments the COD in the raw wastewater ranged from 3175 to 8740 mg $L^{-1}$, showing significant fluctuation, while in the permeate the COD ranged from 17 to 95 mg $L^{-1}$, thus highlighting the excellent removal of organic matter as well as the robustness of the MBR systems. The very similar performance results highlighted no particular differences between the two configurations. The average removal efficiency provided by the AGS compartment was 79.63% (average value between $R_1$ and $R_2$). Therefore, the AGS pre-treatment did not produce any benefit in terms of biological performance. The achieved results, in terms of COD removal, were in general in good agreement with previous applications of MBR for the treatment of high strength wastewater from food industry [36,37], thus confirming the high robustness of MBR towards the abatement of organic loading rates, both soluble and particulate, when treating high strength wastewater. However, most of the application revealed high fouling propensity when treating high strength wastewater [38], as better outlined in a section below.

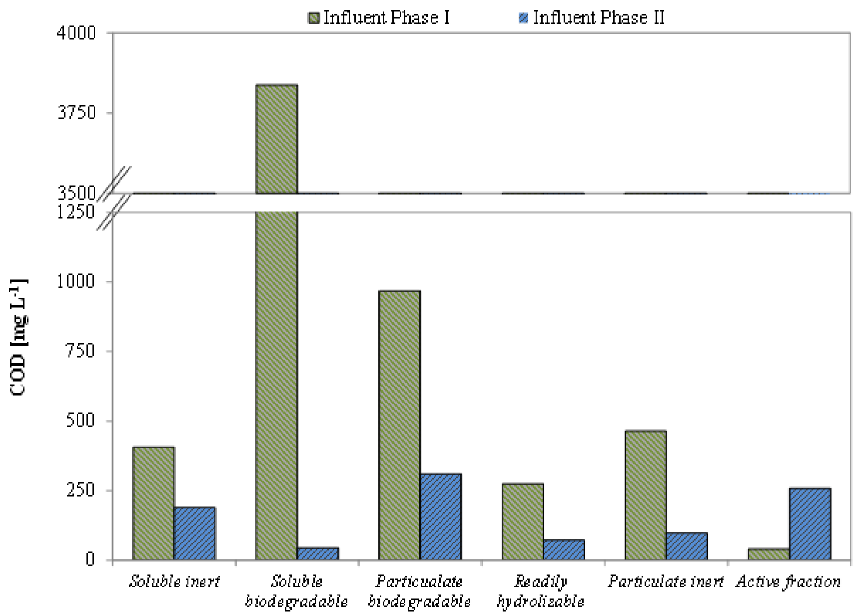


**Figure 3.** COD fractionation results for the influent wastewater to the MBR compartment in Phase I (a) and Phase II (b), respectively.

Referring to COD fractionation, Figure 3 summarizes the typical composition of the feeding wastewater to the MBR compartment. As noticeable from Figure 3, the wastewater fed to the MBR compartment was significantly different for Phase I compared to Phase II. Specifically, the influent wastewater in Phase II was characterized by a lower biodegradability and a greater amount in inert material. Indeed, the soluble biodegradable ($S_S$) COD, corresponding to the readily biodegradable portion of COD (RBCOD) was 67% in Phase I, while it accounted only 5% in Phase II, since it was almost removed during the AGS pre-treatment. In contrast, the particulate biodegradable ($X_S$) COD, representing the slowly biodegradable COD (SBCOD) increased from 22% to 39% in Phase I and II, respectively. As overall, the biodegradable COD (BCOD), expressed as the sum of $S_S$ and $X_S$ decreased from 89% to 44% in Phase I and Phase II, respectively. It is worth noting that the active fraction of biomass in wastewater increased significantly in Phase II, up to 26.54%, while it was only 0.72% in Phase I. This result was likely due to a deterioration of granules physical properties in Phase II that led to a loss of biomass retention capacity in both reactors R1 and R2 [2].

Although the wastewater fed to the MBR during Phase II was characterized by a significantly lower biodegradability, the reactor enabled very high COD removal efficiency. The membrane retention capacity in respect of the particulate organic fraction enabled a longer contact time between microorganisms and pollutants, thereby favouring the onset of hydrolysis phenomena, hence biodegradation of slowly biodegradable organic compounds. Nonetheless, because of metabolic selection of bacteria occurred based on their ability of adapting to the specific wastewater and operating conditions, rather than their ability aggregate in activated sludge flocs or granules, a more effective speciation of bacterial consortium is likely achievable in MBR systems.

This result confirms the value of MBR systems in the field of the treatment of wastewater enriched either in readily biodegradable organic matter or in slowly biodegradable and inert organic fractions. The findings in this study demonstrated a valuable operational flexibility of MBR toward organic loading variations and wastewater compositions, thereby suggesting a real opportunity of full-scale implementation of MBR system in the field of citrus wastewater treatment. The high quality of permeate could also suggest the concrete possibility of effluent permeate internal recycling, thereby promoting fresh-water saving in agreement with the circular economy concepts in the water sector.

### *3.2 Biomass features in the MBR compartment and EPS production/composition*

The features of the biomass consortium in the MBR compartment were evaluated in both Phases by assessing the mixed liquor suspended solid (MLSS) concentrations, EPS production as well as biomass observed yield coefficient ($Y_{obs}$).

In Figure 4 the trend profile of MLSS as well as the VSS/TSS ratio in Phase I (Figure 4a) and Phase II (Figure 4b) is shown.

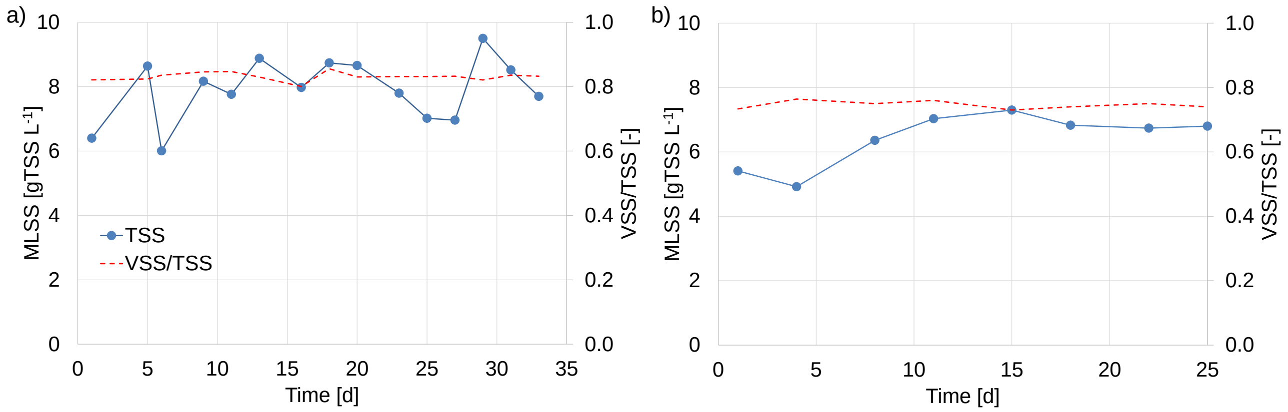


**Figure 4.** Trend profile of MLSS and VSS/TSS in reactor MBR (a) and in MBR compartment of AGS+MBR reactor (b), respectively.

Throughout experiments, the aim was to maintain the MLSS concentration of the MBR compartment in the range 6-8 gTSS $L^{-1}$. From the observation of Figure 4, it is worth noting that the MLSS concentration was higher in Phase I compared to that of Phase II, despite the higher waste flow rates. This is because the higher OLR applied to the MBR compartment in Phase I (average values: 3.8 kgCOD $m^{-3}$ $d^{-1}$ and 0.48 kgCOD $m^{-3}$ $d^{-1}$ in Phase I and Phase II, respectively) promoted a higher growth rate compared to what observed in Phase II. Indeed, the observed Yield coefficient ($Y_{obs}$) was equal to 0.41 gVSS $g^{-1}$COD and 0.35 gVSS $g^{-1}$COD (as average) in Phase I and Phase II, respectively, highlighting that the higher OLR enabled the MLSS enrichment with fast-growing bacteria in Phase I. Moreover, the VSS $TSS^{-1}$ ratio was higher in Phase I (0.83) compared to Phase II (0.75), suggesting the occurrence of inert material accumulation in the MBR compartment in Phase II, likely due to the higher SRT values of the reactor.

Microscopic observations revealed a more compact and firm structure of the activated sludge flocs (Figure 5a) and a higher presence of microfauna (Figure 5b) in the MBR compartment during Phase I. In contrast, in Phase II the mixed liquor was characterized by a more diffuse and weak floc structure (Figure 5c) and a lower presence of microfauna (Figure 5d).

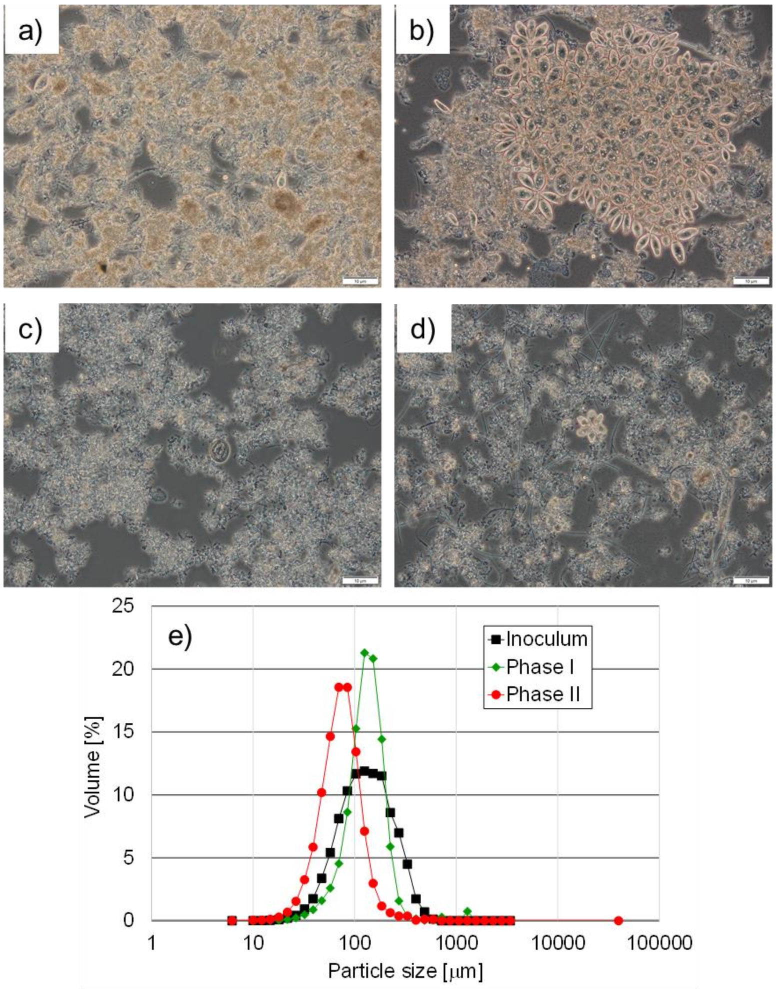


**Figure 5.** Phase contrast observation of activated sludge floc (a) and example of opercularia colony (b) in Phase I; phase contrast micrographs of activated sludge flocs (c-d) in Phase II and particle size distribution (e) throughout experiments.

This result could be also related to the lower biodegradability of the wastewater fed to the MBR compartment that promoted EPS hydrolysis, thus affecting the floc structure. The results of particle size distribution, reported in Figure 5e, confirmed the decrease of the median particle size by volume from Phase I (activated sludge only) to Phase II (activated sludge and crushed granules). This result could have had a potential detrimental effect on fouling tendency in Phase II, referring in particular to the behaviour of the cake layer towards filtration properties, as better outlined in a section below.

Figure 6 reports the trend profile of EPS, in terms of both LB-EPS and TB-EPS as well as the EPS characterization in terms of proteins and polysaccharides in the MBR compartment during Phase I (Figure 6a) and Phase II (Figure 6b), respectively.

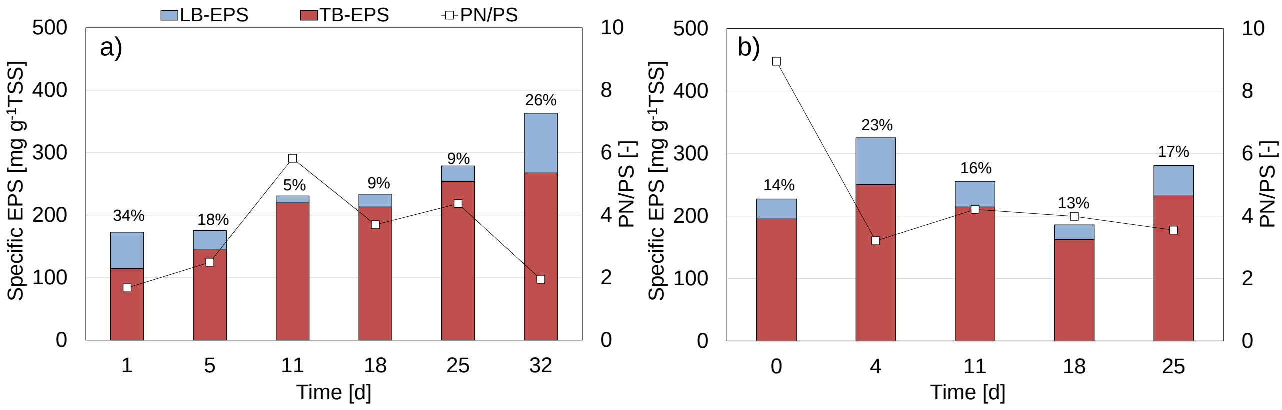


**Figure 6.** Trend profile and composition of EPS in MBR compartment in Phase I (a) and Phase II (b), respectively (the percentage values refer to the LB-EPS content)

From the observation of Figure 6a, it is worth noting a slight increase of specific EPS (referred to g of TSS) during Phase I, from 173 mgEPS $g^{-1}$TSS to 360 mgEPS $g^{-1}$TSS, while in Phase II the EPS concentration showed a slight decrease and remaining close to an average value of 255 mgEPS $g^{-1}$TSS (Figure 6b). This behaviour is in agreement previous studies revealing a decrease of bound EPS with an increase of SRT [39]. In both phases, the TB-EPS fraction was the main component of EPS by more than 83%, whilst the LB-EPS accounted for less than 17%. Concerning TB-EPS, proteins were the main component in Phase I with average values of 78%. In Phase II, it was observed a slight increase of the TB-EPS protein content within the MBR compartment, up to 88%. In contrast, the LB-EPS showed a different trend, highlighting a decrease of the protein content from 56% to 45% in Phase I and Phase II respectively, corresponding to a polysaccharides increase from 44% to 55%. Moreover, the different content/composition of ESP might be also related to the SRT increase in the MBR compartment during Phase II. This result could have influenced the fouling mechanisms in terms of reversible portion, as better outlined in a section below.

*3.3 Biomass respiratory activity, kinetic/stoichiometric behaviour*

As aforementioned, respirometric batch tests were carried out for assessing the kinetic/stoichiometric parameters of heterotrophic species throughout experiments. In general, the achieved respirogram charts followed the typical exogenous (after external substrate spiking) and endogenous (after substrate exhaustion) respiration phases. Table 2 summarizes the average values of kinetic/stoichiometric parameters achieved during experiments. The biomass samples subjected to respirometric analysis were collected from the MBR compartment.

**Table 2.** Average values of the main kinetic/stoichiometric parameters in the MBR compartment assessed during experiments (in brackets the standard deviation values)

| Parameter | Units | Phase I (MBR) | Phase II (AGS+MBR) |
|---|---|---|---|
| $\mathbf{Y_H}$ | [mgCOD mg$^{-1}$COD] | 0.63 (±0.11) | 0.69 (±0.01) |
| $\mathbf{Y_{STO}}$ | [mgCOD mg$^{-1}$COD] | 0.81 (±0.11) | 0.83 (±0.03) |
| $\mu_{H,max}$ | [d$^{-1}$] | 2.86 (±1.31) | 4.69 (±2.02) |
| **Ks** | [mgCOD L$^{-1}$] | 21.51 (±10.30) | 13.02 (±6.95) |
| **SOUR** | [mg$O_2$ g$^{-1}$SSV d$^{-1}$] | 27.59 (±8.45) | 33.28 (±12.38) |
| $\mathbf{b_H}$ | [d$^{-1}$] | 0.29 (±0.09) | 0.21 (±0.08) |
| **FA** | [%] | 31.00 (±3.85) | 27.53 (±16.84) |

As noticeable from Table 2, the heterotrophic population showed a good activity level, with kinetic/stoichiometric parameters well in the range of what reported in the technical literature for MBR systems [40–42]. The heterotrophic species showed high activity levels, since the MBR plant start-up. This result is likely due to the seeding sludge, collected from a real wastewater treatment plant yet acclimated to this kind of wastewater. No significant differences were noticed throughout experiments, with active heterotrophic fractions (FA) equal to 31 and 27% in Phase I and Phase II, respectively. These high values were likely due to the high OLR applied to the pilot plants, referring in particular to Phase I. Nevertheless, as noticeable from Table 2 the heterotrophic activity was more pronounced in Phase II, with slight higher values of the yield coefficient $Y_H$, heterotrophic growth rate $\mu_{H,max}$, and specific respiration rates (SOUR). Based on the above results, it could be stated that the pre-treatment of wastewater did not result in significant change in the biomass metabolic activity. Despite the decrease in the biodegradable organic fraction of the influent fed occurred during Phase II, biomass showed a metabolic behaviour fully comparable with that observed in the previous experimental phase. This result could be likely related to a deterioration of the granules structure occurring in Phase II with the release in the bulk liquid (subsequently fed to the MBR compartment) of high active biomass. This circumstance is confirmed by the very high specific substrate depletion rate observed in the AGS reactors, as outlined by [2]. Although the heterotrophic active fraction was slightly lower during Phase II in the MBR (27.5% *vs* 31)%, it should be recalled that the SRT was significantly higher (38 days *vs* 9.2 days). Under these operating conditions, it should expected a lower biomass active fraction, because of prevailing of bacterial decay phenomena on new bacterial cells synthesis [43]. Therefore, it is reasonable that enrichment in biomass active fraction deriving from the AGS pre-treatment reactors enabled to achieve a positive net grow, thereby balancing the bacterial decay due to the high SRT with an “external” supply of new biomass.

Moreover, it was noticed the occurrence of the “storage” phenomenon, due to the ability of specific microorganisms to accumulate the external substrate as internal storage products (polyhydroxyalkoanates and/or polyhydroxybutyrate). Such phenomenon is highlighted through a typical “tail” in the respirogram chart [44] and the storage yield coefficient $Y_{STO}$ was assessed according to the procedure proposed in the literature [45,46].

*3.4 Analysis of membrane fouling*

Figure 7 depicts the trend profile of total resistance ($R_T$) (Figure 7a-b) and membrane permeability (Figure 7c-d) in Phase I and II, respectively.

Regarding Phase I, excepting the first days after MBR start-up, the $R_T$ showed a regular and moderate increase up to experimental day 12, when a rapid worsening of the filtration ability was observed (TMP increase) (Figure 7a). Afterwards, two physical cleanings where carried out at day 16 and day

22 to control the fouling tendency, but the filtration recovery was only limited, likely due to pore blocking increase. This result could suggest that the membrane fouling was mainly irreversible. Therefore, at day 27 and 33, two chemical cleanings were carried out, that enabled to recover most of the filtration ability of the physical membrane. Indeed, the permeability recovery was much higher with chemical actions than with physical cleaning operations.

Nevertheless, $R_T$ was lower compared to that of Phase II (Figure 7b). This result was confirmed by the trend profile of membrane permeability assessed during experiments (Figure 7c-d).

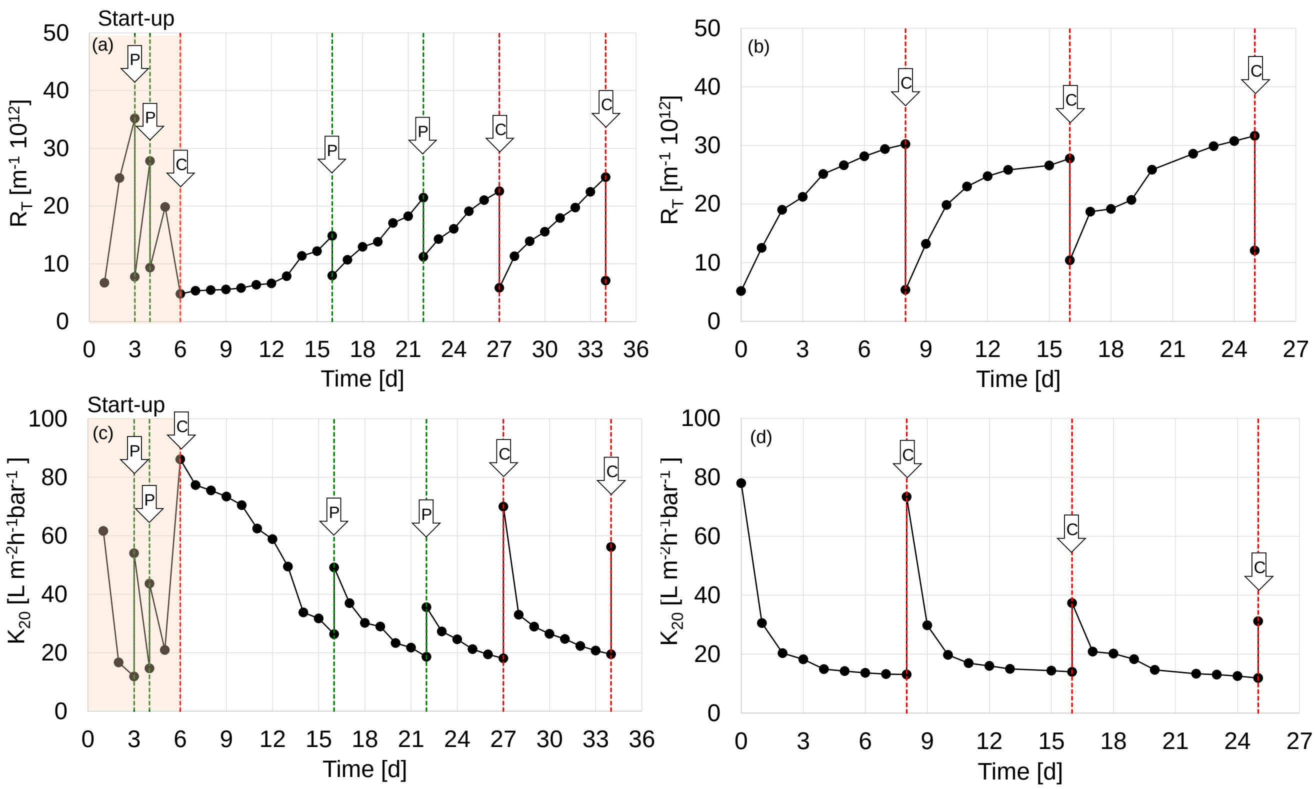


**Figure 7.** Trend profile of total resistance in Phase I (a) and Phase II (b), time course of membrane permeability in Phase I (c) and Phase II (c), respectively (in the arrows, “P” standing for physical and “C” for chemical cleaning).

Indeed, in Phase II it was observed a rapid increase of $R_T$ in the first days after membrane cleaning operations (Figure 7b), likely due to a very fast particles deposition on membrane surface, leading to a rapid increase of resistance due to cake formation. The peculiar features of the mixed liquor in Phase II likely promoted the development of a cake layer that enhanced the membrane fouling [14].

Thereafter, the observed $R_T$ increase was less pronounced. The fouling rate (FR) showed a quite moderate and regular trend in Phase I, with values almost lower than 5 $10^{12}$ $m^{-1}$ $d^{-1}$ (Figure 8a); in contrast, in Phase II it was observed a rapid increase of FR immediately after membrane cleaning operations (Figure 8b) in good agreement with the $R_T$ trend, achieving values close to 10 $10^{12}$ $m^{-1}$ $d^{-1}$. The results obtained in Phase II indicated that the bulk, consisting of activated sludge and crushed granules from the AGS reactor, showed a more pronounced tendency to deposit on the membrane surface in the short-term than the activated sludge alone. It can be speculated that the presence of the crushed granules contributed to increase the overall bulk hydrophobicity in the AGS+MBR system, because of the higher hydrophobicity which distinguishes the granular sludge from the flocculent activated sludge. The sludge deriving from the granular sludge detachment is also denser than activated sludge. Accordingly, cake layer constituted by granules and activated sludge can maintain a relatively stable form throughout the filtration process compared to the activated sludge alone, which is more prone to be compressed as the filtration proceeds [47]. For these reasons, it is reasonable assuming that the lower compressibility of the cake layer formed by crushed granules and activated sludge led to rapid increase in TMP at the beginning of filtration and gradual increase in TMP subsequently. this results is in good agreement with the findings of Ao et al. (2018). Therefore, the filtration resistance proceeded more slowly in the long-term in the AGS+MBR system than the MBR.

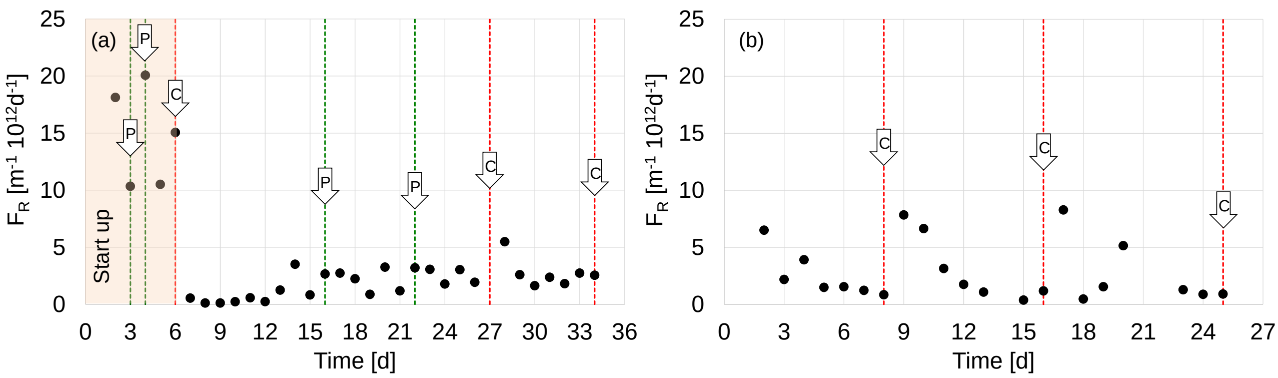


**Figure 8.** Time course of membrane fouling rate in Phase I (a) and Phase II (b), respectively (in the arrows, "P" standing for physical and "C" for chemical cleaning).

As aforementioned, the RIS model application during membrane cleaning operations enabled to assess the specific fouling mechanisms, according to Di Bella et al. (2018). The results of RIS model application are summarized in Figure 8. Concerning Phase I (Figure 9a), the main fouling mechanism was the resistance due to irreversible cake deposition ($R_{C,irr}$), defined in the present study as the portion of cake layer not removable by ordinary cleaning actions (i.e membrane backflushing with permeate), but removable almost completely with extraordinary physical actions (i.e. membrane water washing).

Nevertheless, the percentage contribution of $R_{C,irr}$ showed a gradual decrease during experiments. In contrast, the percentage contribution of $R_{PB}$ slightly increased from 0.7% to 26.42% from Day 3 to Day 22, indicating that the frequency of chemical cleaning operations should be increased for the treatment of this high strength wastewater and under the explored operational conditions. Indeed, according to literature [9] it was assumed that the resistance due to pore blocking ($R_{PB}$) is not removable by physical actions (either ordinary or extraordinary), but it can be partially removed through chemical actions only.

Referring to Phase II (Figure 9b), it was noticed a different behaviour. Indeed, although the main fouling mechanism remained the $R_{C,irr}$, it showed a slight decrease throughout experiments and it was also observed a decrease of the pore blocking contribution (from 41.20% to 25.92%) and a significant increase of reversible cake contribution (from 8.95% to 28.52%) at Day 8 and Day 35, respectively.

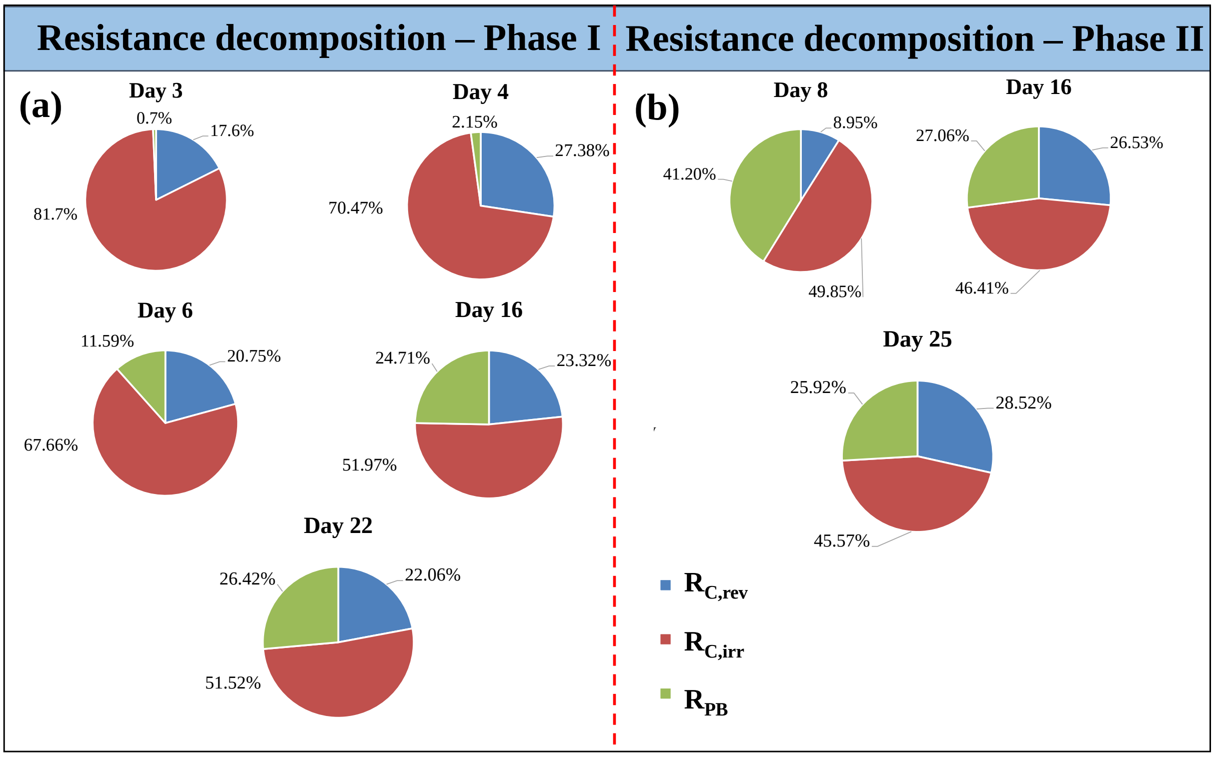


**Figure 9.** Resistance decomposition through RIS model and percentage contribution in Phase I (a) and Phase II (b), respectively.

From the achieved results, a first sight might suggest a better behaviour of the AGS+MBR system in terms of fouling development and reversibility. However, it has to be stressed that the residual resistance ($R_{Res}$) after chemical cleaning operations (i.e. the irremovable fouling resistance that cannot be removed even with chemicals) showed a different behaviour in Phase II compared to Phase I (Figure 10). Indeed, it was observed a much higher increase of irremovable resistance ($R_{Res}$) in Phase II compared to Phase I; this result is of paramount importance, since it might severely influence the membrane filtration ability, thus leading to a reduced service life in the middle/long period. The above results clearly indicated that the pore-blocking mechanism in the AGS+MBR system was more severe than that in the only MBR with activated sludge. It is reasonable that the mixture of activated sludge and crushed aerobic granules generated a more hydrophobic cake layer that rapidly deposited on the membrane surface, thereby resulting in a rapid increase in the $R_T$ in the short-term. At the same time, being the cake layer less compressible, filtration resistance proceeded more slowly in the long-term

[48]. Moreover, as reported in the literature [49], the cake layer in the AGS+MBR system was likely more porous because of the presence of bigger particles, deriving from the AGS rector, thereby resulting in a higher number of pore canals. In such condition, the mass transport of soluble proteins and carbohydrates within the membrane pores could be enhanced. Furthermore, the reduced C/N ratio in the MBR compartment, coupled to the presence of particles deriving from granules deterioration in Phase II, could have promoted the increase of polysaccharides in LB-EPS and a decrease of particle size, giving rise to higher irreversible fouling resistance. This result is in good agreement with previous studies [50]. Moreover, the lower biodegradability of the wastewater fed to the MBR compartment, coupled to the higher SRT, could have enhanced the EPS hydrolysis.

Basing on the above results, the AGS+MBR configuration, while not providing any significant beneficial effect in terms of COD removal, promoted a deterioration of membrane filtration properties in the MBR compartment. In this light, a careful management of the AGS should be carried out in order to ensure granules stability and successfully apply the in-series treatment AGS+MBR. Otherwise a coagulation-UF (CUF) pre-treatment could be suggested to protect the membrane module from irreversible fouling [51]. Therefore, the applicability of AGS+MBR configuration for high strength wastewater treatment should be carefully verified and further studies are needed to confirm the findings of the present study.

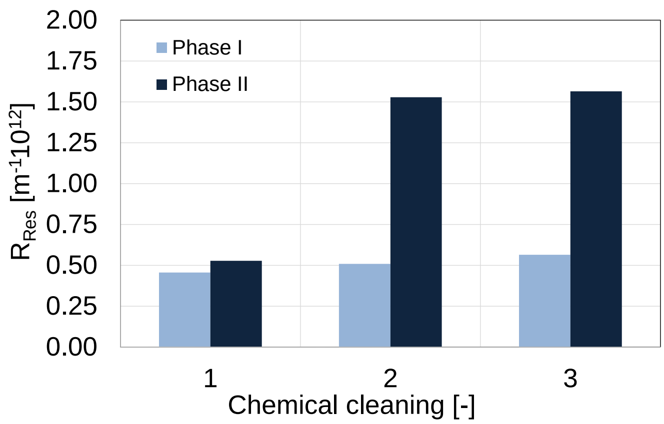


**Figure 10.** Residual (irremovable) resistance trend after chemical cleaning actions in Phase I and II, respectively.

Concerning the specific fouling mechanisms, by analysing the effect of EPS content on membrane fouling, it was observed an interesting behaviour (Figure 11). Indeed, in Phase I it was observed a not negligible correlation between the resistance due to cake deposition (both reversible and irreversible) and the polysaccharide content in the TB-EPS (Figure 11a). This result could have promoted a gel formation on the surface membrane, increasing significantly the resistance to filtration. However, a chemical action under alkaline conditions could contribute to remove this jelly fouling [22]. Indeed, the fouling due to polysaccharides is usually more “reversible” compared to that produced by humic substances or proteins.

In contrast, in Phase II it was observed a relationship between the presence of proteins in the SMP and the resistance due to pore blocking (Figure 11b). This situation is of importance, since SMP can enter more easily in the membrane pores, thus contributing to establish an irremovable fouling and to a permanent loss of membrane permeability [52]. Nevertheless, these first results need to be confirmed in future experimental activities, characterized by longer durations.

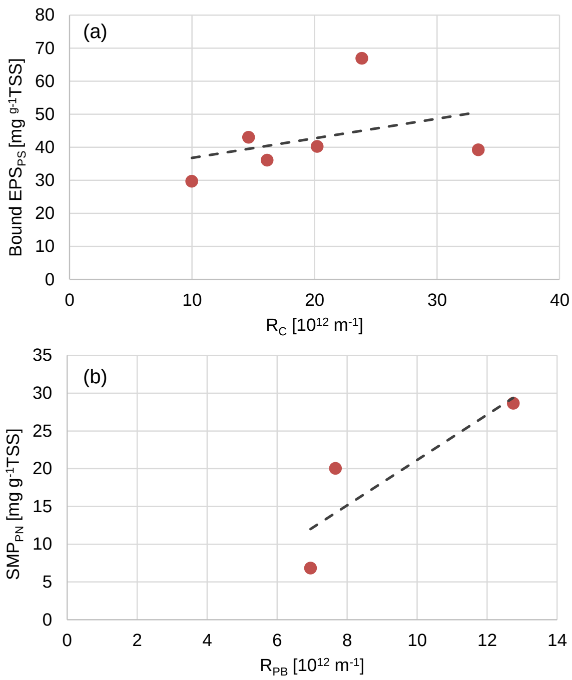


**Figure 11.** Relationship between cake resistance and TB-EPS polysaccharides in Phase I (a) and between resistance to pore blocking and SMP proteins in Phase II (b).

## 4. Conclusions

The present study was aimed at investigating the effect of AGS pre-treatment in MBR plants when treating high strength citrus wastewater, especially in terms of fouling behaviour. The AGS+MBR was characterized by higher values of total resistance to filtration, likely due to a rapid deposition on the membrane surface. The worsening of granules stability, with decrease of the average size of the crushed granules, could have emphasized this behaviour. Moreover, the AGS+MBR configuration was characterized by a higher increase of irremovable fouling that can shorten the membrane life. In this light, for the investigated operational conditions, the pre-treatment with AGS was not advisable. Nevertheless, further research activity is needed on this topic, since AGS+MBR configuration might have great potentiality (if granules stability and proper granule size is ensured) due to the extreme compactness of the AGS compartment as well as the energy saving and the much richer biological community within the granules (with anaerobic, aerobic and aerobic internal structure). Moreover, the use of membrane compartment as tertiary filtration of the AGS effluent even applying a coagulation treatment (CUF) prior to membrane filtration should be also explored. Finally, the quality of the membrane permeate would meet the requirements for water reuse, thus promoting a cleaner and more sustainable operation of the citrus processing industry.

## Acknowledgments

Authors thank "Agrumaria Corleone S.p.A." (Palermo) for the precious technical support. Furthermore, authors warmly thank Eng. Carlo Liborio “Boris” Adriano for his valuable contribution during pilot plant operations.

## References

[1] D.A. Zema, S. Andiloro, G. Bombino, V. Tamburino, R. Sidari, A. Caridi, Depuration in aerated ponds of citrus processing wastewater with a high concentration of essential oils,

Environ. Technol. 33 (2012) 1255–1260. doi:10.1080/09593330.2011.618938.

[2] S.F. Corsino, D. Di Trapani, M. Torregrossa, G. Viviani, Aerobic granular sludge treating high strength citrus wastewater: Analysis of pH and organic loading rate effect on kinetics, performance and stability, J. Environ. Manage. 214 (2018) 23–35. doi:10.1016/j.jenvman.2018.02.087.

[3] R.O. Cristóvão, C.M. Botelho, R.J.E. Martins, J.M. Loureiro, R.A.R. Boaventura, Fish canning industry wastewater treatment for water reuse – a case study, J. Clean. Prod. 87 (2015) 603–612. doi:10.1016/j.jclepro.2014.10.076.

[4] L. Yan, X. Ye, R.J. Linhardt, J. Chen, D. Yu, R. Huang, D. Liu, S. Chen, Full recovery of value-added compounds from citrus canning processing water, J. Clean. Prod. 176 (2018) 959–965. doi:10.1016/j.jclepro.2017.12.018.

[5] A.R. Navarro, Z.O. Lopez, M.C. Maldonado, A pilot plant for the treatment of lemon industry wastewater, Clean Technol. Environ. Policy. 10 (2008) 371–375. doi:10.1007/s10098-008-0152-9.

[6] H. El-Kamah, A. Tawfik, M. Mahmoud, H. Abdel-Halim, Treatment of high strength wastewater from fruit juice industry using integrated anaerobic/aerobic system, Desalination. 253 (2010) 158–163. doi:10.1016/j.desal.2009.11.013.

[7] The Council of the European Union, COUNCIL DIRECTIV 98/83/EC, 2000. doi:2004R0726 - v.7 of 05.06.2013.

[8] D.A. Zema, P.S. Calabrò, A. Folino, V. Tamburino, G. Zappia, S.M. Zimbone, Valorisation of citrus processing waste: A review, Waste Manag. 80 (2018) 252–273. doi:10.1016/j.wasman.2018.09.024.

[9] G. Di Bella, D. Di Trapani, S. Judd, Fouling mechanism elucidation in membrane bioreactors

by bespoke physical cleaning, Sep. Purif. Technol. 199 (2018) 124–133. doi:10.1016/j.seppur.2018.01.049.

[10] G. Mannina, M. Capodici, A. Cosenza, D. Di Trapani, G.A. Ekama, The effect of the solids and hydraulic retention time on moving bed membrane bioreactor performance, J. Clean. Prod. 170 (2018) 1305–1315. doi:10.1016/j.jclepro.2017.09.200.

[11] S. Judd, C. Judd, The MBR book, 2006. doi:10.1016/B978-1-85617-481-7.X5000-4.

[12] M.C. Collivignarelli, A. Abbà, F. Castagnola, G. Bertanza, Minimization of municipal sewage sludge by means of a thermophilic membrane bioreactor with intermittent aeration, J. Clean. Prod. 143 (2017) 369–376. doi:10.1016/j.jclepro.2016.12.101.

[13] A. Cosenza, G. Di Bella, G. Mannina, M. Torregrossa, The role of EPS in fouling and foaming phenomena for a membrane bioreactor, Bioresour. Technol. 147 (2013) 184–192. doi:10.1016/j.biortech.2013.08.026.

[14] J. Xiong, D. Fu, R.P. Singh, J.J. Ducoste, Structural characteristics and development of the cake layer in a dynamic membrane bioreactor, Sep. Purif. Technol. 167 (2016) 88–96. doi:10.1016/j.seppur.2016.04.040.

[15] G. Mannina, M. Capodici, A. Cosenza, D. Di Trapani, G. Olsson, Greenhouse gas emissions and the links to plant performance in a fixed-film activated sludge membrane bioreactor – Pilot plant experimental evidence, Bioresour. Technol. 241 (2017) 1145–1151. doi:10.1016/j.biortech.2017.05.043.

[16] W.J. Gao, M.N. Han, X. Qu, C. Xu, B.Q. Liao, Characteristics of wastewater and mixed liquor and their role in membrane fouling, Bioresour. Technol. 128 (2013) 207–214. doi:10.1016/j.biortech.2012.10.075.

[17] M.K. de Kreuk, N. Kishida, S. Tsuneda, M.C.M. van Loosdrecht, Behavior of polymeric

substrates in an aerobic granular sludge system, Water Res. 44 (2010) 5929–5938. doi:10.1016/j.watres.2010.07.033.

[18] L. Liu, G.P. Sheng, W.W. Li, Z.H. Tong, R.J. Zeng, J.X. Liu, J. Xie, S.C. Peng, H.Q. Yu, Cultivation of aerobic granular sludge with a mixed wastewater rich in toxic organics, Biochem. Eng. J. 57 (2011) 7–12. doi:10.1016/j.bej.2011.07.005.

[19] S.F. Corsino, R. Campo, G. Di, M. Torregrossa, International Biodeterioration & Biodegradation Cultivation of granular sludge with hypersaline oily wastewater, Int. Biodeterior. Biodegradation. 105 (2015) 192–202. doi:10.1016/j.ibiod.2015.09.009.

[20] M. Pronk, B. Abbas, S.H.K. Al-zuhairy, R. Kraan, R. Kleerebezem, M.C.M. van Loosdrecht, Effect and behaviour of different substrates in relation to the formation of aerobic granular sludge, Appl. Microbiol. Biotechnol. 99 (2015) 5257–5268. doi:10.1007/s00253-014-6358-3.

[21] A. Val del Río, M. Figueroa, B. Arrojo, A. Mosquera-Corral, J.L. Campos, G. García-Torriello, R. Méndez, Aerobic granular SBR systems applied to the treatment of industrial effluents, J. Environ. Manage. 95 (2012) S88–S92. doi:10.1016/j.jenvman.2011.03.019.

[22] F. Meng, S. Zhang, Y. Oh, Z. Zhou, H.-S. Shin, S.-R. Chae, Review Fouling in membrane bioreactors: An updated review, Water Res. 114 (2017) 151–180. doi:10.1016/J.WATRES.2017.02.006.

[23] Z. Wang, H. Yu, J. Ma, X. Zheng, Z. Wu, Recent advances in membrane bio-technologies for sludge reduction and treatment, Biotechnol. Adv. 31 (2013) 1187–1199. doi:10.1016/j.biotechadv.2013.02.004.

[24] S.F. Corsino, R. Campo, G. Di Bella, M. Torregrossa, G. Viviani, Study of aerobic granular sludge stability in a continuous-flow membrane bioreactor, Bioresour. Technol. 200 (2016) 1055–1059. doi:10.1016/j.biortech.2015.10.065.

[25] W. Zhang, F. Jiang, Membrane fouling in aerobic granular sludge (AGS)-membrane bioreactor (MBR): effect of AGS size, Water Res. (2018). doi:10.1016/j.watres.2018.07.069.

[26] M. Noronha, T. Britz, V. Mavrov, H.D. Janke, H. Chmiel, Treatment of spent process water from a fruit juice company for purposes of reuse: Hybrid process concept and on-site test operation of a pilot plant, Desalination. 143 (2002) 183–196. doi:10.1016/S0011-9164(02)00239-4.

[27] S.F. Corsino, M. Capodici, M. Torregrossa, G. Viviani, Fate of aerobic granular sludge in the long-term: The role of EPSs on the clogging of granular sludge porosity, J. Environ. Manage. 183 (2016). doi:10.1016/j.jenvman.2016.09.004.

[28] E. Cetin, E. Karakas, E. Dulekgurgen, S. Ovez, M. Kolukirik, G. Yilmaz, Effects of high-concentration influent suspended solids on aerobic granulation in pilot-scale sequencing batch reactors treating real domestic wastewater, Water Res. (2018). doi:10.1016/j.watres.2017.12.014.

[29] Apha, Standard Methods for the Examination of Water & Wastewater, 2005.

[30] G. Mannina, M. Capodici, A. Cosenza, D. Di Trapani, Carbon and nutrient biological removal in a University of Cape Town membrane bioreactor: Analysis of a pilot plant operated under two different C/N ratios, Chem. Eng. J. 296 (2016) 289–299. doi:10.1016/j.cej.2016.03.114.

[31] O.H. Lowry, N.J. Rosebrough, L. Farr, R. Randall, Protein measurement with the folin phenol reagent, J. Biol. Chem. 193 (1951) 265–275. doi:10.1016/0304-3894(92)87011-4.

[32] M. DuBois, K. a. Gilles, J.K. Hamilton, P. a. Rebers, F. Smith, Colorimetric method for determination of sugars and related substances, Anal. Chem. 28 (1956) 350–356. doi:10.1021/ac60111a017.

[33] M. Torregrossa, G. Di Bella, D. Di Trapani, Comparison between ozonation and the OSA process: Analysis of excess sludge reduction and biomass activity in two different pilot plants, Water Sci. Technol. 66 (2012) 185–192. doi:10.2166/wst.2012.153.

[34] M. Capodici, S. Fabio Corsino, F. Di Pippo, D. Di Trapani, M. Torregrossa, An innovative respirometric method to assess the autotrophic active fraction: Application to an alternate oxic–anoxic MBR pilot plant, Chem. Eng. J. 300 (2016) 367–375. doi:10.1016/j.cej.2016.04.134.

[35] A. Robles, M. V. Ruano, J. Ribes, J. Ferrer, Factors that affect the permeability of commercial hollow-fibre membranes in a submerged anaerobic MBR (HF-SAnMBR) system, Water Res. 47 (2013) 1277–1288. doi:10.1016/j.watres.2012.11.055.

[36] H. Harada, K. Momonoi, S. Yamazaki, S. Takizawa, Application of anaerobic-UF membrane reactor for treatment of a wastewater containing high strength particulate organics, in: Water Sci. Technol., 1994: pp. 307–319.

[37] N.S.A. Mutamim, Z.Z. Noor, M.A.A. Hassan, G. Olsson, Application of membrane bioreactor technology in treating high strength industrial wastewater: A performance review, Desalination. 305 (2012) 1–11. doi:10.1016/j.desal.2012.07.033.

[38] S.M. Tauseef, T. Abbasi, S.A. Abbasi, Energy recovery from wastewaters with high-rate anaerobic digesters, Renew. Sustain. Energy Rev. 19 (2013) 704–741. doi:10.1016/j.rser.2012.11.056.

[39] F. Meng, S.R. Chae, A. Drews, M. Kraume, H.S. Shin, F. Yang, Recent advances in membrane bioreactors (MBRs): Membrane fouling and membrane material, Water Res. 43 (2009) 1489–1512. doi:10.1016/j.watres.2008.12.044.

[40] G. Munz, R. Gori, L. Cammilli, C. Lubello, Characterization of tannery wastewater and

biomass in a membrane bioreactor using respirometric analysis, Bioresour. Technol. 99 (2008) 8612–8618. doi:10.1016/j.biortech.2008.04.004.

[41] H. Hauduc, L. Rieger, T. Ohtsuki, A. Shaw, I. Takács, S. Winkler, A. Héduit, P.A. Vanrolleghem, S. Gillot, Activated sludge modelling: Development and potential use of a practical applications database, Water Sci. Technol. 63 (2011) 2164–2182. doi:10.2166/wst.2011.368.

[42] G. Di Bella, D. Di Trapani, M. Torregrossa, G. Viviani, Performance of a MBR pilot plant treating high strength wastewater subject to salinity increase: Analysis of biomass activity and fouling behaviour, Bioresour. Technol. 147 (2013) 614–618. doi:10.1016/j.biortech.2013.08.025.

[43] M. Majewsky, T. Gallé, V. Yargeau, K. Fischer, Active heterotrophic biomass and sludge retention time (SRT) as determining factors for biodegradation kinetics of pharmaceuticals in activated sludge, Bioresour. Technol. 102 (2011) 7415–7421. doi:10.1016/j.biortech.2011.05.032.

[44] M. Capodici, S. Fabio Corsino, F. Di Pippo, D. Di Trapani, M. Torregrossa, An innovative respirometric method to assess the autotrophic active fraction: Application to an alternate oxic-anoxic MBR pilot plant, Chem. Eng. J. 300 (2016). doi:10.1016/j.cej.2016.04.134.

[45] A. Carucci, D. Dionisi, M. Majone, E. Rolle, P. Smurra, Aerobic storage by activated sludge on real wastewater, Water Res. 35 (2001) 3833–3844. doi:10.1016/S0043-1354(01)00108-7.

[46] Ö. Karahan-Gül, N. Artan, D. Orhon, M. Henze, M.C.M. Van Loosdrecht, Respirometric assessment of storage yield for different substrates, in: Water Sci. Technol., 2002: pp. 345–352.

[47] W. Jing-Feng, Q. Zhi-Gang, C. Zhi-Qiang, L. Jun-Wen, Z. Yi-Hong, W. Xuan, Z. Bin,

Comparison and analysis of membrane fouling between flocculent sludge membrane bioreactor and granular sludge membrane bioreactor, PLoS One. 7 (2012). doi:10.1371/journal.pone.0040819.

[48] L. Ao, W. Liu, M. Zhang, X. Wang, Analysis of effect of particles on cake layer compressibility during ultrafiltration of upflow biological activated carbon effluent, Sci. Total Environ. 619–620 (2018) 232–238. doi:10.1016/j.scitotenv.2017.11.002.

[49] J. ZHOU, F. lin YANG, F. gang MENG, P. AN, D. WANG, Comparison of membrane fouling during short-term filtration of aerobic granular sludge and activated sludge, J. Environ. Sci. 19 (2007) 1281–1286. doi:10.1016/S1001-0742(07)60209-5.

[50] L. Deng, W. Guo, H.H. Ngo, H. Zhang, J. Wang, J. Li, S. Xia, Y. Wu, Biofouling and control approaches in membrane bioreactors, Bioresour. Technol. 221 (2016) 656–665. doi:10.1016/j.biortech.2016.09.105.

[51] W. Yu, L.C. Campos, N. Graham, Application of pulsed UV-irradiation and pre-coagulation to control ultrafiltration membrane fouling in the treatment of micro-polluted surface water, Water Res. 107 (2016) 83–92. doi:10.1016/j.watres.2016.10.058.

[52] H. Lin, M. Zhang, F. Wang, F. Meng, B.Q. Liao, H. Hong, J. Chen, W. Gao, A critical review of extracellular polymeric substances (EPSs) in membrane bioreactors: Characteristics, roles in membrane fouling and control strategies, J. Memb. Sci. 460 (2014) 110–125. doi:10.1016/j.memsci.2014.02.034.

## FIGURE CAPTIONS

**Figure 1.** Schematic lay-out of (a) MBR and (b) in-series AGS+MBR configurations.

**Figure 2.** Influent, supernatant MLSS and permeate COD concentrations and removal efficiencies in Phase I (a) organic loading rate applied and removed in Phase I (b) and influent, supernatant MLSS and permeate COD concentrations and removal efficiencies in Phase II (c) organic loading rate applied and removed in Phase II (d), respectively.

**Figure 3.** COD fractionation results for the influent wastewater to the MBR compartment in Phase I (a) and Phase II (b), respectively.

**Figure 4.** Trend profile of MLSS and VSS/TSS in reactor MBR (a) and in MBR compartment of AGS+MBR reactor (b), respectively.

**Figure 5.** Phase contrast observation of activated sludge floc (a) and example of opercularia colony (b) in Phase I; phase contrast micrographs of activated sludge flocs (c-d) in Phase II and particle size distribution (e) throughout experiments.

**Figure 6.** Trend profile and composition of EPS in MBR compartment in Phase I (a) and Phase II (b), respectively (the percentage values refer to the LB-EPS content)

**Figure 7.** Trend profile of total resistance in Phase I (a) and Phase II (b), time course of membrane permeability in Phase I (c) and Phase II (c), respectively (in the arrows, "P" standing for physical and "C" for chemical cleaning).

**Figure 8.** Time course of membrane fouling rate in Phase I (a) and Phase II (b), respectively (in the arrows, "P" standing for physical and "C" for chemical cleaning).

**Figure 9.** Resistance decomposition through RIS model and percentage contribution in Phase I (a) and Phase II (b), respectively.

**Figure 10.** Residual (irremovable) resistance trend after chemical cleaning actions in Phase I and II, respectively.

**Figure 11.** Relationship between cake resistance and TB-EPS polysaccharides in Phase I (a) and between resistance to pore blocking and SMP proteins in Phase II (b).

## TABLE LEGENDS

**Table1.** Main characteristics of the raw wastewater as well as operational conditions (in brackets the standard deviation values)

**Table 2.** Average values of the main kinetic/stoichiometric parameters in the MBR compartment assessed during experiments (in brackets the standard deviation values)